Author(s): Al-Rasheed, Hessa H.; AL-khamis, Sarah A.; Barakat, Assem; El-Faham, Ayman; Haukka, Matti; Soliman, Saied M.

Title: Synthesis and Characterizations of Novel Isatin-s-Triazine Hydrazone Derivatives : X-ray Structure, Hirshfeld Analysis and DFT Calculations

Year: 2023

Version: Published version

crystals

MDPI

Article

Synthesis and Characterizations of Novel Isatin-*s*-Triazine Hydrazone Derivatives; X-ray Structure, Hirshfeld Analysis and DFT Calculations

Hessa H. Al-Rasheed [1], Sarah A. AL-khamis [1], Assem Barakat [1], Ayman El-Faham [2,*], Matti Haukka [3] and Saied M. Soliman [2,*]

[1] Department of Chemistry, College of Science, King Saud University, P.O. Box 2455, Riyadh 11451, Saudi Arabia
[2] Department of Chemistry, Faculty of Science, Alexandria University, P.O. Box 426, Ibrahimia, Alexandria 21321, Egypt
[3] Department of Chemistry, University of Jyväskylä, P.O. Box 35, FI-40014 Jyväskylä, Finland
* Correspondence: ayman.elfaham@alexu.edu.eg (A.E.-F.); saeed.soliman@alexu.edu.eg (S.M.S.)

Abstract: A novel series of isatin-*s*-triazine hydrazone derivatives has been synthesized and reported herein. The synthetic methodology involved the reaction of *s*-triazine hydrazine precursors with isatin derivatives in the presence of CH_3COOH as a catalyst and EtOH as solvent to afford the corresponding target products 6a-e in high yields and purities. The characterization data obtained from elemental analysis, FT-IR, NMR (^{1}H- and ^{13}C-) were in full agreement with the expected structures. Furthermore, an X-ray single crystal diffraction study of one of the target *s*-triazine hydrazone derivatives, 6c confirmed the structure of the desired compounds. It crystallized in the triclinic crystal system and *P-1* space group with a = 10.3368(6) Å, b = 11.9804(8) Å, c = 12.7250(5) Å, α = 100.904(4)°, β = 107.959(4)° and γ = 109.638(6)°. The different non-covalent interactions which contributed in the molecular packing of 6c were analyzed using Hirshfeld analysis. The molecular packing of the organic part of the crystal structure showed important O ... H (7.1%), C ... H (16.4%), C ... C (1.6%), H ... H (34.8%), N ... H (8.0%) and C ... N (4.0%) interactions while for the crystal solvent, the O ... H (21.3%), H ... H (61.2%) and N ... H (8.1%) contacts are the most significant. The studied compound 6c is polar and has a net dipole moment of 5.6072 Debye based on DFT study.

Keywords: *s*-triazine; isatin; hydrazone derivatives; Hirshfeld; DFT; non-covalent interactions

Citation: Al-Rasheed, H.H.; AL-khamis, S.A.; Barakat, A.; El-Faham, A.; Haukka, M.; Soliman, S.M. Synthesis and Characterizations of Novel Isatin-*s*-Triazine Hydrazone Derivatives; X-ray Structure, Hirshfeld Analysis and DFT Calculations. *Crystals* **2023**, *13*, 305. https://doi.org/10.3390/cryst13020305

Academic Editor: Alexander Y. Nazarenko

Received: 28 January 2023
Revised: 4 February 2023
Accepted: 9 February 2023
Published: 12 February 2023

1. Introduction

s-Triazine derivatives have attracted the attention of many researchers due to their remarkable uses in a variety of sectors, including those in the pharmaceutical industry, polymers, and corrosion inhibitors [1–3]. The substantial biological activity of substituted *s*-triazine derivatives, such as their antibacterial, antifungal, antimalarial, anticancer, anti-inflammatory, and antileishmanial effects, have made them desirable candidates in medicinal chemistry [4–10].

On the other hand, isatin derivatives have diverse applications in biology and pharmaceutics [11,12]. Additionally, isatin derivatives are considered as starting materials for the synthesis of many heterocycles [13,14]. These compounds are also used as anticancer, antibiotic and antidepressant [15–20]. Shanmugakala et al. reported some metal complexes of indolin-3-one/1,3,5-triazine hybrid as organic ligand. The in vivo studies revealed a potential anticonvulsant as well as anti-inflammatory actions of these complexes [21].

In continuation to our interest in developing a new *s*-triazine hydrazone derivatives with isatin to explore new derivatives of compounds incorporated the two moieties, *s*-triazine and istain, with hydrazone linkage. The supramolecular structural properties of one of the synthesized *s*-triazine derivatives **6c** were explored using single crystal X-ray

diffraction analysis augmented with Hirshfeld calculations. Additionally, DFT calculations were performed to analyze the molecular and electronic aspects of this compound.

2. Experimental

2.1. Materials and Methods

All materials and methods details are given in Method S1 (Supplementary Data).

2.2. Synthetic Methodology

Synthesis of the compounds **2**–**4** was performed using the reported method [22] and their spectral characterizations are described in details in Method S2 (Supplementary Data).

2.2.1. General Method for the Synthesis of 1,3,5-Triazine-Hydrazone Derivatives, **6a–e**

Substituted isatin **5a–e** (2 mmoles) was dissolved in 30 mL ethanol and 2–3 drops of acetic acid (AcOH). Then *s*-triazine hydrazine **4** (2 mmoles) was added portion wise on the hot solution and stirred. After complete addition, the reaction mixture was refluxed for 3–4 h (the reaction followed by TLC using ethylacetate-hexane 2:1). At the end, the reaction was left to cool slowly to room temperature and then the product was collected by filtration, washed with cold ethanol, and dried to produce the pure products, as indicated from the spectral data.

Synthesis of 3-(2-(4-((4-Chlorophenyl)amino)-6-(piperidin-1-yl)-1,3,5-triazin-2-yl)hydrazineylidene)indolin-2-one, **6a**

The product was obtained as a white solid in yield 94%; mp 254–256 °C; IR (KBr, cm^{-1}): 3281 (NH), 1581(C=N), 1488, 1412 (C=C); ^{1}H NMR (DMSO-d_6): δ = 1.49 (s, 4H, 2CH2), 1.59 (s, 2H, CH_2), 3.72 (d, *J* = 62.1 Hz, 4H, $2CH_2$), 7.06–6.88 (m, 4H, 4CH), 7.47–7.46 (m, 3H, 3CH), 7.74 (s, 1H, CH), 9.75 (s, 1H, NH), 11.26 (s, 1H, NH-CO), 12.56 (s, 1H, NH-N=) ppm; ^{13}C NMR (DMSO-d_6): δ = 24.2, 25.4, 43.9, 64.3, 110.9, 119.9, 120.4, 121.2, 122.5, 125.6, 128.4, 130.4, 132.9, 138.9, 141.3, 163.1, 163.9 ppm. Anal. Calc. for $C_{22}H_{21}ClN_8O$ (448.91): C, 58.86; H, 4.72; N, 24.96. Found: C, 58.99; H, 4.65; N, 24.87.

5-Bromo-3-(2-(4-((4-Chlorophenyl)amino)-6-(piperidin-1-yl)-1,3,5-triazin-2-yl)hydrazineylidene)indolin-2-one, **6b**

The product was obtained as a yellow solid in yield 92%; mp 290–291 °C; IR (KBr, cm−1): 3151 (NH), 1581(C=N), 1486, 1412 (C=C); ^{1}H NMR (DMSO-d_6): δ = δ1.45 (d, *J* = 65.0 Hz, 4H, $2CH_2$), 1.66 (m, 2H, CH2),3.81–3.59 (m, 4H, 2CH2), 6.7 (m, 4H, 4CH), 7.38–7.15 (m, 2H, 2CH), 7.5 (s, 1H, CH), 9.5 (s, 1H, NH), 11.11 (s, 1H, NH-CO), 12.32 (s, 1H, NH-N=) ppm; ^{13}C NMR (DMSO-d_6): δ = 24.2, 25.4, 59.7, 112.9, 114.0, 121.1, 121.9, 122.6, 125.6, 128.3, 131.6, 132.4, 138.86, 140.3, 162.6, 163.7, 164.2, 170.3 ppm. Anal. Calc. for $C_{22}H_{20}BrClN_8O$ (527.80): C, 50.06; H, 3.82; N, 21.23. Found C, 50.23; H, 3.95; N, 21.51.

5-Chloro-3-(2-(4-((4-Chlorophenyl)amino)-6-(piperidin-1-yl)-1,3,5-triazin-2-yl)hydrazineylidene)indolin-2-One, **6c**

The product was obtained as a yellow solid in yield 99%; mp 291–293 °C; IR (KBr, cm^{-1}): 3291 (NH), 1582(C=N), 1488, 1418 (C=C); ^{1}H NMR (DMSO-d_6): δ = 1.49 (s, 4H, 2CH2), 1.59 (s, 2H, CH_2), 3.71 (m, 4H, 2CH2), 6.9–6.88 (m, 4H, 4CH), 7.38–7.2 (m, 2H, 2CH), 7.72 (s, 1H, CH), 9.73 (s, 1H, NH), 11.26 (s, 1H, NH-CO), 12.48 (s, 1H, NH-N=) ppm; ^{13}C NMR (DMSO-d_6): δ = 24.2, 25.5, 43.9, 112.44, 119.3, 121.1, 121.2, 122.2, 125.6, 126.5, 128.3, 129.7, 131.8, 138.9, 139.94, 162.9, 163.7, 164.2, 172.1 ppm. Anal. Calc. for $C_{22}H_{20}Cl_2N_8O$ (483.35): C, 54.67; H, 4.17; N, 23.18. Found C, 54.89; H, 4.31; N, 23.36.

3-(2-(4-((4-Chlorophenyl)amino)-6-(piperidin-1-yl)-1,3,5-triazin-2-yl)hydrazineylidene)-5-fluoroindolin-2-one, **6d**

The product was obtained as a yellow solid in yield 93%; mp 276–278 °C; IR (KBr, cm^{-1}): 3220 (NH), 1582(C=N), 1486, 1420 (C=C); ^{1}H NMR (DMSO-d_6): δ = 1.49 (s, 4H,

$2CH_2$), 1.59 (s, 2H, CH_2), 3.72 (m, 4H, $2CH_2$), 7.21–6.87 (m, 4H, 4CH), 7.31–7.29 (m, 2H, 2CH), 7.73 (s, 1H, CH), 9.73 (s, 1H, NH), 11.17 (s, 1H, NH-CO), 12.57 (s, 1H, NH-N=) ppm; ^{13}C NMR (DMSO-d_6): δ = 24.2, 25.4, 43.9, 106.8, 106.9, 111.9, 112.0, 116.6, 116.8, 121.2, 121.7, 125.6, 128.4, 132.4, 137.6, 138.9, 157.3, 159.2, 163.2, 163.8, 164.2,172.0 ppm. Anal. Calc. for C22H20ClFN8O (466.90): C, 56.59; H, 4.32; N, 24.00. Found C, 56.71; H, 4.48; N, 24.23.

3-(2-(4-((4-Chlorophenyl)amino)-6-(piperidin-1-yl)-1,3,5-triazin-2-yl)hydrazineylidene)-5-methylindolin-2-one, **6e**

The product was obtained as a yellow solid in yield 77%; mp 296–297 °C; IR (KBr, cm^{-1}): 3287 (NH), 1581 (C=N), 1494, 1422 (C=C); ^{1}H NMR (DMSO-d_6): δ = 1.49 (s, 4H, 2CH2), 1.59 (s, 2H, CH2), 2.26 (s, 3H, CH3), 3.72 (m, 4H, 2CH2), 7.26–6.76 (m, 4H, 4CH), 7.30–7.29 (m, 2H, 2CH), 7.72 (s, 1H, CH), 9.73 (s, 1H, NH), 11.05 (s, 1H, NH-CO), 12.55 (s, 1H, NH-N=) ppm; ^{13}C NMR (DMSO-d_6): δ = 24.2, 25.4, 43.9, 106.8, 107.0, 112.0, 112.0, 116.6, 116.8, 121.2, 121.8, 125.6, 128.4, 132.4, 137.6, 138.9, 157.4, 159.2, 163.2, 163.8, 164.2, 172.1 ppm. Anal. Calc. for $C_{23}H_{23}FN_8O$ (446.48): C, 61.87; H, 5.19; N, 25.10. Found C, 61.96; H, 5.32; N, 25.35.

2.3. X-ray Structure Determinations

The crystal of 6c was solved using the method described in Method S3 (Supplementary Data) [23–26]. The crystallographic details are summarized in Table 1.

Table 1. Crystal data for **6c**.

	6c
CCDC	2214508
empirical formula	$C_{26}H_{28}Cl_2N_8O_3$
Fw	571.46
temp (K)	120(2)
λ (Å)	0.71073
cryst syst	Triclinic
space group	P $\bar{1}$
a (Å)	10.3368(6)
b (Å)	11.9804(8)
c (Å)	12.7250(5)
α (deg)	100.904(4)
β (deg)	107.959(4)
γ(deg)	109.638(6)
V (Å^3)	1334.36(14)
Z	2
ρ_{calc} (Mg/m^3)	1.422
μ (Mo Kα) (mm^{-1})	0.289
No. reflns.	12754
Unique reflns.	7212
Completeness to θ = 67.684°	100%
GOOF (F^2)	1.031
R_{int}	0.0286
R_1 [a] ($I \geq 2\sigma$)	0.0482
wR_2 [b] ($I \geq 2\sigma$)	0.0953

[a] $R_1 = \Sigma||F_o| - |F_c||/\Sigma|F_o|$. [b] $wR_2 = \{\Sigma[w(F_o^2 - F_c^2)^2]/\Sigma[w(F_o^2)^2]\}^{1/2}$.

2.4. Hirshfeld and DFT Computations

The details of the topology [27] and DFT [28–30] calculations are summarized in Method S4 (Supplementary Data).

3. Results and Discussion

3.1. Synthesis and Characterizations

The initial step for the synthesis of the target products involved the reaction of cyanuric chloride **1** with *p*-chloroaninline via nucleophilic aromatic substitution of one of the chlorine atoms at 0 °C in the presence of the alkaline medium of $NaHCO_3$ following the previously reported method [22] to afford the derivative **2**. The second step involved a further displacement of the second chlorine atom by piperidine as a nucleophile at room temperature to give the derivative **3** [22] in a good yield and purity, as indicated from the spectral data (Supporting Information, Figures S1 and S2). Then, the derivative **3** was treated with hydrazine hydrate (80%) in ethanol overnight under reflux to afford the hydrazine derivative **4**, which reacted directly without further purification with isatin derivatives **5a–e** in ethanol as a solvent in the presence of catalytic amount of acetic acid to afford the products **6a–e** in good yield and purities (Scheme 1).

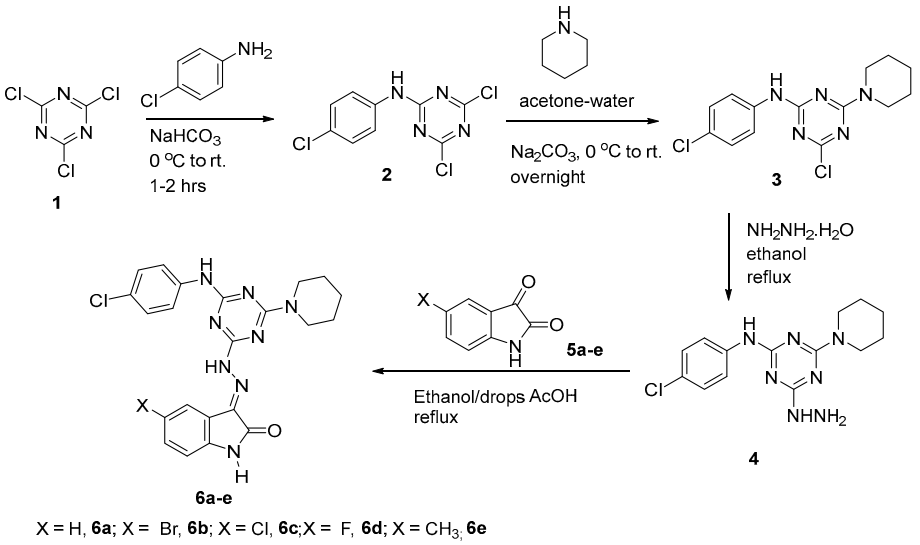

Scheme 1. Synthetic route for preparation of *s*-triazine hydrazone derivatives.

3.2. X-ray Structure Description

The structure of **6c** is presented in Figure 1. Its crystal system is triclinic and the space group is *P-1*. The asymmetric unit comprised one molecule of the target compound and a co-crystallized ethyl acetate as a crystal solvent. The triclinic parameters are a = 10.3368(6) Å, b = 11.9804(8) Å, c = 12.7250(5) Å, α = 100.904(4)°, β =107.959(4)° and γ = 109.638(6)°. The unit cell volume is 1334.36 $Å^3$ while the calculated density is 1.422 mg/m^3 (Table 1). The target compound comprising one *s*-triazine core with three different substituents attached to the 2, 4 and 6 positions. The *s*-triazine core has almost planar structure where the CNCN dihedral angles do not exceed 5.1° (C14N3C8N2). The 1,3,5-triazine ring makes an angle of 14.78 and 5.99° with the aryl and indole moieties, respectively. The former showed a larger twist with respect to the triazine moiety compared to the latter. For the piperidine moiety, the ring showed a clear chair configuration. The most important geometrical parameters are listed in Table 2 and Table S1.

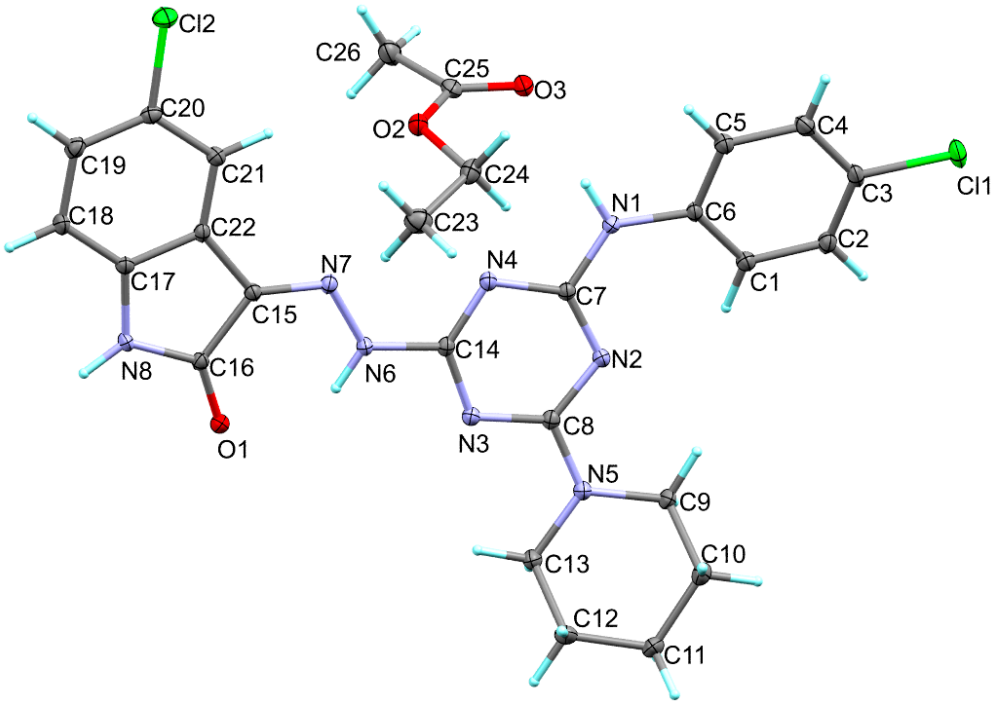

Figure 1. X-ray structure of **6c**.

Table 2. Selected bond lengths [Å] for **6c** [a].

Atoms	Distance	Atoms	Distance
Cl1-C3	1.746	N4-C7	1.3592
Cl2-C20	1.7472	N5-C8	1.3462
O1-C16	1.2352	N5-C13	1.4632
N1-C7	1.3632	N5-C9	1.4652
N1-C6	1.4132	N6-N7	1.3352
N2-C7	1.3292	N6-C14	1.3862
N2-C8	1.3502	N7-C15	1.3012
N3-C14	1.3322	N8-C16	1.3622
N3-C8	1.3502	N8-C17	1.3982
N4-C14	1.3252		

[a] List of bond angles in **6c** are given in Table S1 Supplementary Data.

The X-ray structure of the titled compound showed a molecule of ethylacetate as a crystal solvent where both molecules are stabilized by some intra-molecular interactions including the classical N1-H1...O3 hydrogen bond and the non-classical C21-H21...O2 interactions, where the N1 . . . O3 and C21...O2 distances are 2.931(2) and 3.433(3) Å, respectively. In addition, the crystal solvent shared in the packing scheme of 6c by the intermolecular C26-H26A...N3 interaction with C26...N3 distance of 3.461(3) Å. The donor(D)-hydrogen(H) . . . acceptor(A) angles are 149, 175(2) and 159°, respectively. Additionally, the molecules of the target compound are connected with each other via strong and classical N8-H8...O1 hydrogen bonds where the H . . . A and D . . . A distances are 1.98 and 2.854(2) Å, respectively, while the D-H . . . A angle is 170°. It is worth noting that the structure of the target organic molecule showed numerous intra-molecular interactions including the non-classical C-H . . . N interactions and the classical N6-H6 . . . O1 hydrogen bond (Figure 2). List of these contacts are depicted in Table 3 while the packing scheme of this compound is shown in Figure 3.

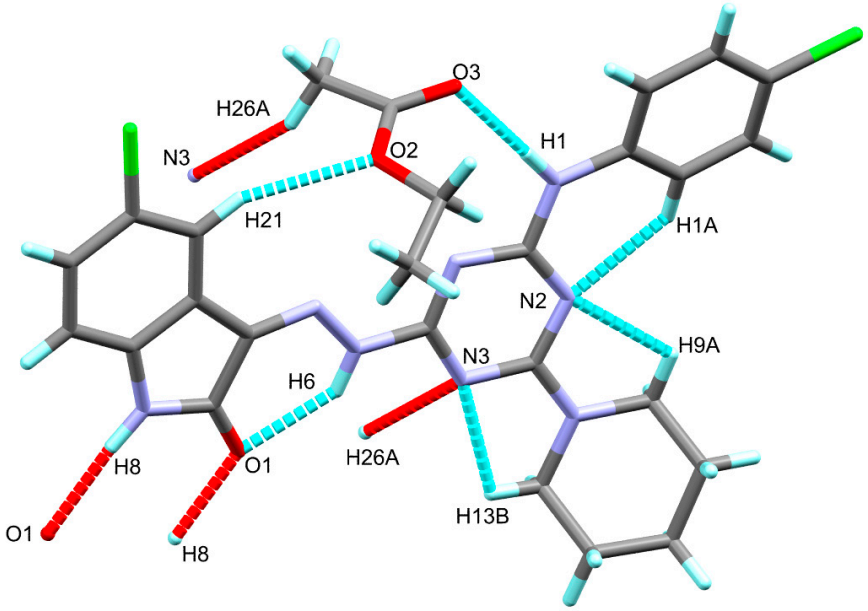

Figure 2. Possible intra- and intermolecular contacts in **6c**.

Table 3. Hydrogen bonds for **6c** [Å and °].

D-H...A	d(D-H)	d(H . . . A)	d(D . . . A)	<(DHA)	Symm. Codes
N1-H1 . . . O3	0.88(2)	2.05(2)	2.931(2)	175(2)	
C21-H21 . . . O2	0.95	2.53	3.433(3)	159	
N6-H6 . . . O1	0.88	2.04	2.755(2)	137	
N8-H8 . . . O1	0.88	1.98	2.854(2)	170	2-x, 1-y, 1-z
C1-H1A . . . N2	0.95	2.35	2.922(3)	118	
C9-H9A . . . N2	0.99	2.31	2.750(3)	106	
C13-H13B . . . N3	0.99	2.31	2.747(3)	106	
C26-H26A . . . N3	0.98	2.59	3.461(3)	149	1-x, 1-y, 1-z

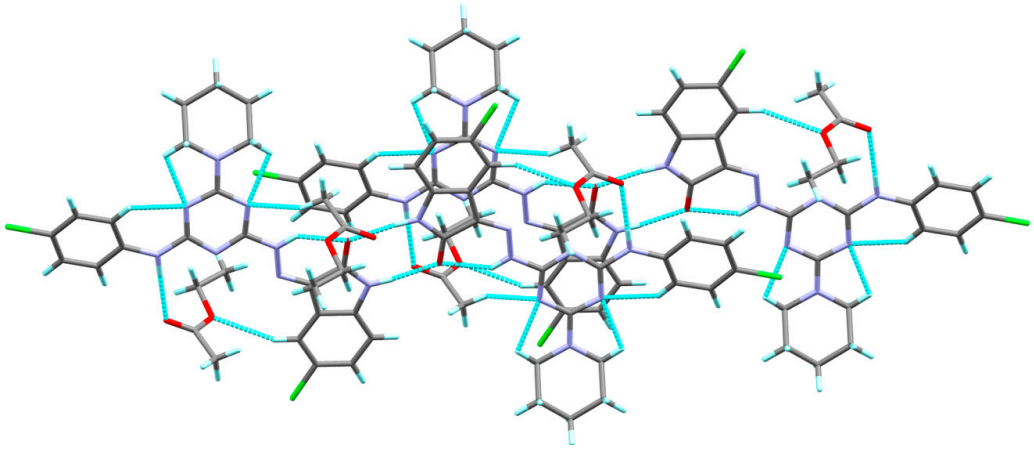

Figure 3. Molecular packing showing the intra- and inter-molecular C-H . . . O and C-H . . . N interactions.

3.3. Hirshfeld Surface Analysis

There are many weak and strong intra- and inter-molecular interactions in the crystal structure of **6c**. These non-covalent interactions could be simply analyzed using Hirshfeld calculations. The resulting d_{norm}, shape index and curvedness maps as well as the fingerprint plot could give a full picture not only about all possible non-covalent interactions but also about the contributions of all these contacts. The studied crystal structure comprised

one molecule of the target organic compound and one ethylacetate as a crystal solvent per asymmetric unit. Hence, the Hirshfeld surfaces were performed for each molecule and the resulting maps are collected in Figure 4.

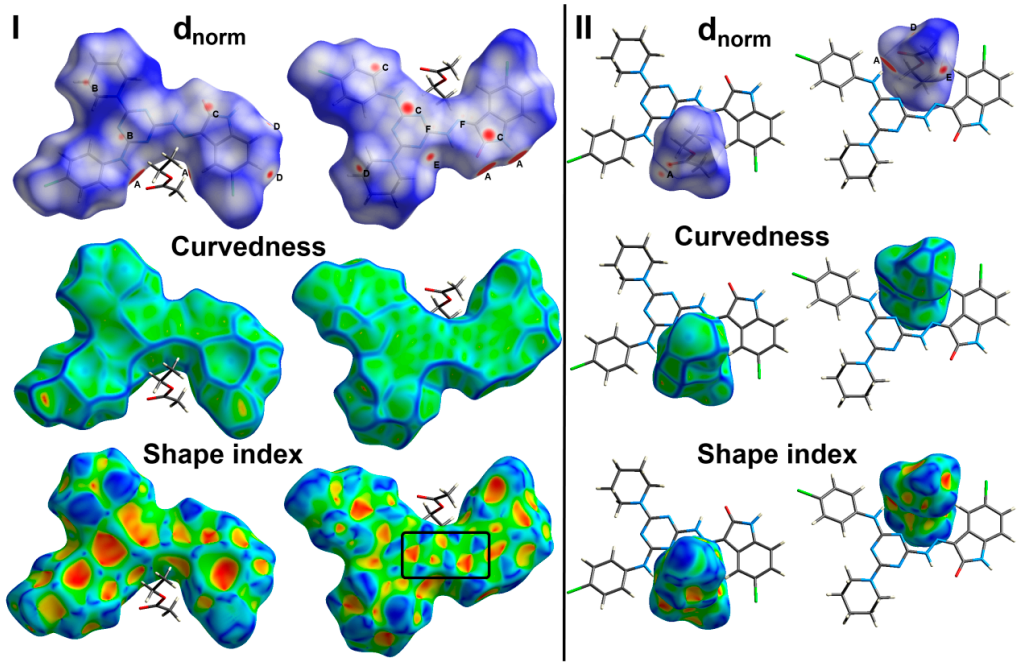

Figure 4. Hirshfeld surfaces for the target molecule (**I**) and the crystal solvent (**II**) showing the most significant contacts; A, B, C, D, E and F refer to the short O . . . H, C . . . H, C . . . C, H . . . H, N . . . H and C . . . N interactions, respectively.

The most significant contacts appeared as red spots in the d_{norm} map. For simplicity, these contacts are labelled in Figure 4 by letters A to E which corresponds to the O . . . H, C . . . H, C . . . C, H . . . H, N . . . H and C . . . N contacts, respectively. The decomposed d_{norm} maps and fingerprint plots of these interactions are presented in Figures 5 and 6 for the target organic molecule and the crystal solvent, respectively. The red regions could be detected close to the atoms which share significant interactions with other molecules outside the surface. For the target organic molecule, there are many O...H contacts occurred between the surface and the surrounding molecules. The O2 . . . H21 (2.408 Å) and O3 . . . H1 (1.925 Å) interactions occur between the organic target molecule and the crystal solvent. In addition, there are O3 . . . H24A (2.513 Å) and O1 . . . H8 (1.857 Å) short contacts. The former occurs between two molecules of the crystal solvent while the latter occurs between two of the target organic molecule. The N3 . . . H26A contact (2.498 Å) is another polar interaction is found to occur between the N3 atom of the *s*-triazine core and H26A from the crystal solvent. In addition, other non-polar contacts such as C . . . H, H . . . H and C . . . C interactions were detected. The C . . . H contacts which belong to the C-H . . . π interaction occurred between C7 atom of the *s*-triazine core and H10B from the piperidine moiety where the corresponding C7 . . . H10B interaction distance is 2.712 Å. On the other hand, the most important hydrogenic interactions are H18 . . . H26B (2.103 Å) and H19 . . . H9B (2.058 Å). The former occurs between H18 from the organic target molecule and H26B from the crystal solvent while the latter occurs between H19 and H9B from two neighboring units of the organic target molecule. Interestingly, the Hirshfeld analysis detected many C . . . C and C . . . N contacts which reveal the presence of some interactions between the π-system of the studied molecule. The C5 . . . C16 (3.299 Å), C7 . . . C16 (3.218 Å), C14 . . . C15 (3.388 Å) and C14 . . . N7 (3.230 Å) are the most important. All these π-π interactions occur between two of the organic target molecules. The π-π interactions appeared as red/blue

triangles in the shape index map and green flat area in curvedness. For better clarity, the regions included in the π-π interactions are marked by black rectangle in Figure 4.

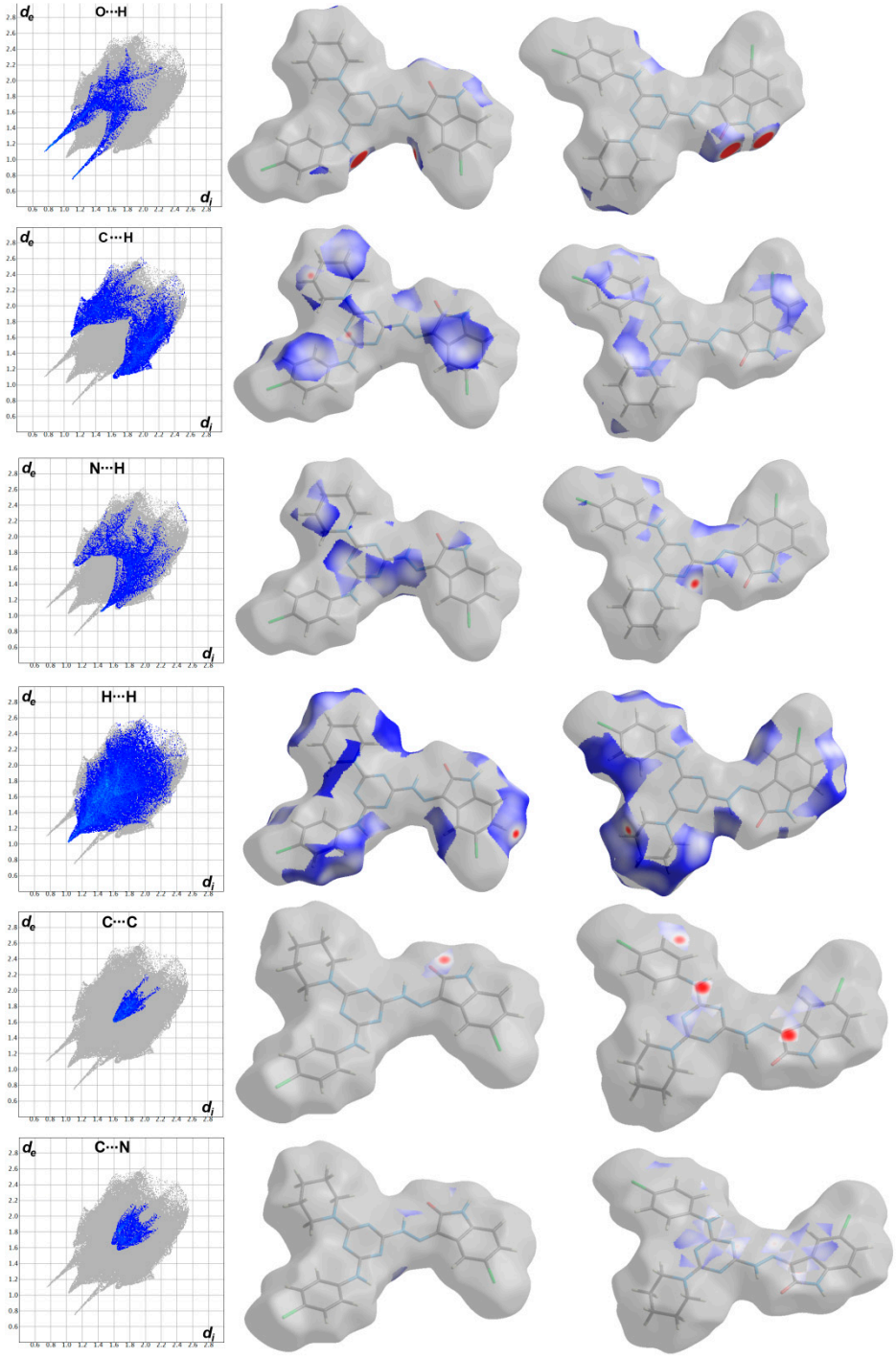

Figure 5. The fingerprint plots and d_{norm} maps for the important contacts in the target molecule in the crystal structure of **6c**.

In addition, the area of the decomposed fingerprint plots of the O . . . H, C . . . H, C . . . C, H . . . H, N . . . H and C . . . N interactions represents the contribution of this contact in the molecular packing (Figure 5). For the organic target molecule, the percentages of these contacts are 7.1, 16.4, 1.6, 34.8, 8.0 and 4.0, respectively. In the case of the crystal solvent, the Hirshfeld analysis of this part of the crystal structure indicated the importance of the O . . . H, H . . . H and N . . . H contacts (Figure 6). Their percentages are 21.3, 61.2 and 8.1%,

respectively. There are many other contracts presented along with their percentages are summarized in Figure 7. These interactions have low importance in the molecular packing compared to the above-mentioned contacts.

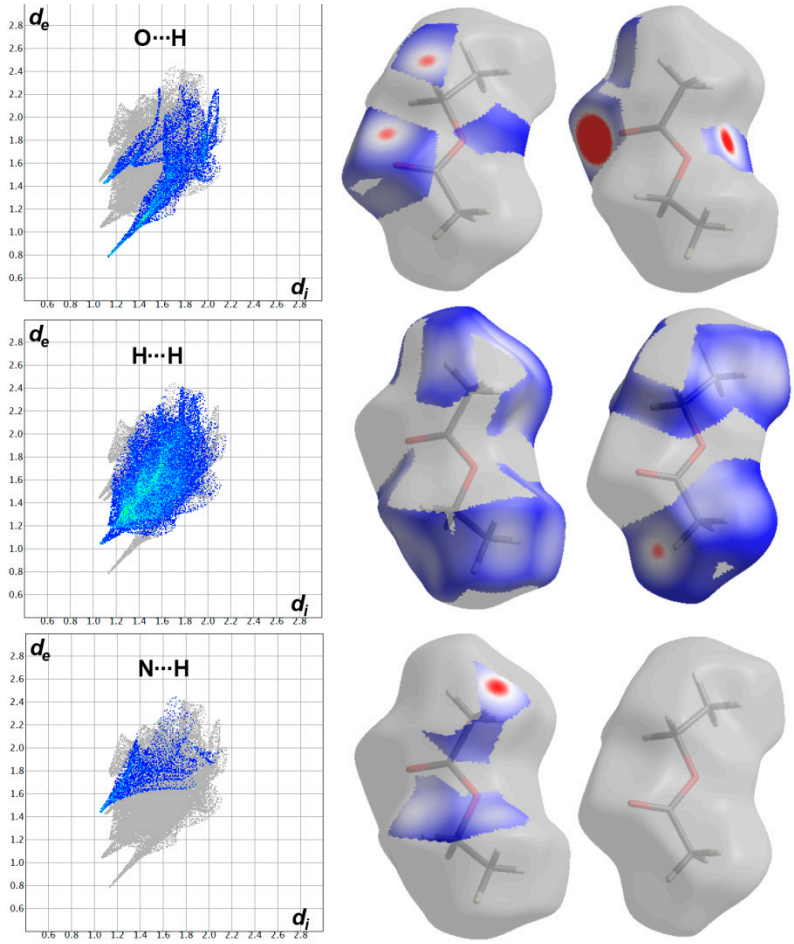

Figure 6. The fingerprint plots and d_{norm} maps for the short contacts in the crystal solvent in the crystal structure of **6c**.

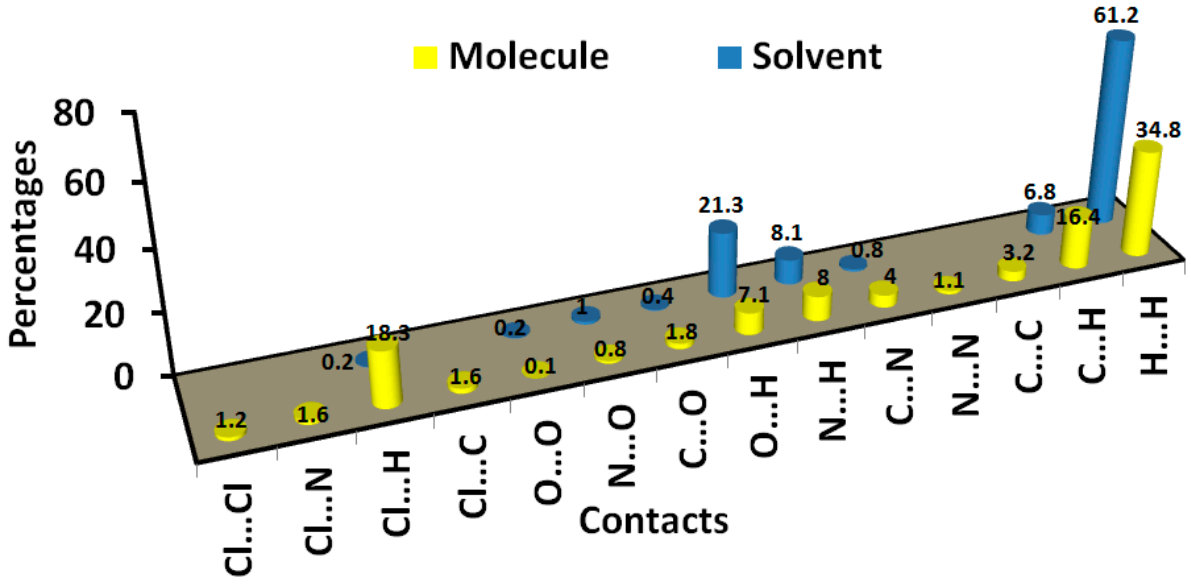

Figure 7. Intermolecular contacts and their percentages in **6c**.

3.4. DFT Analyses

The calculated structure of 6c is shown in Figure 8A. In the same figure, the overlay of the X-ray structure over the calculated one is shown in Figure 8B. There is general great agreement between both structures. Additionally, there are good correlations between the calculated and optimized geometric parameters (Figure 9). List of the bond distances and angles are collected in Table S2 (Supplementary Data).

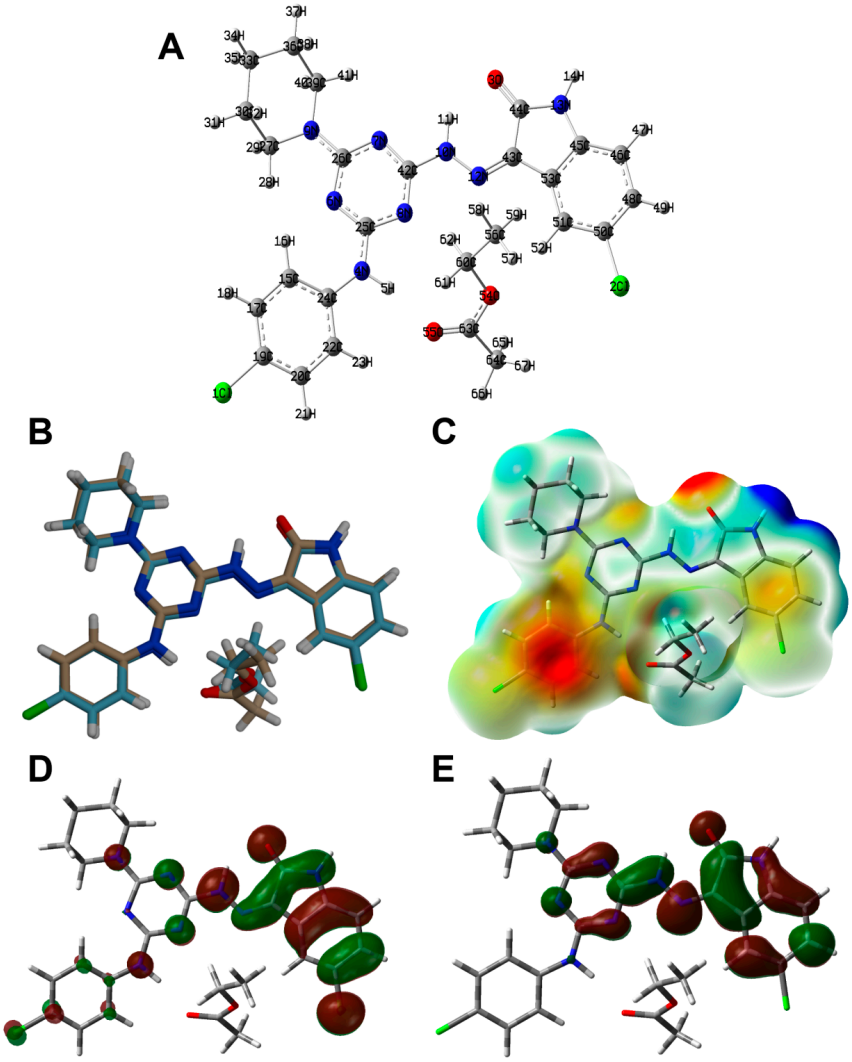

Figure 8. Optimized geometry (**A**), overlay with the X-ray geometry (**B**), MEP (**C**), HOMO (**D**) and LUMO (**E**) of **6c**.

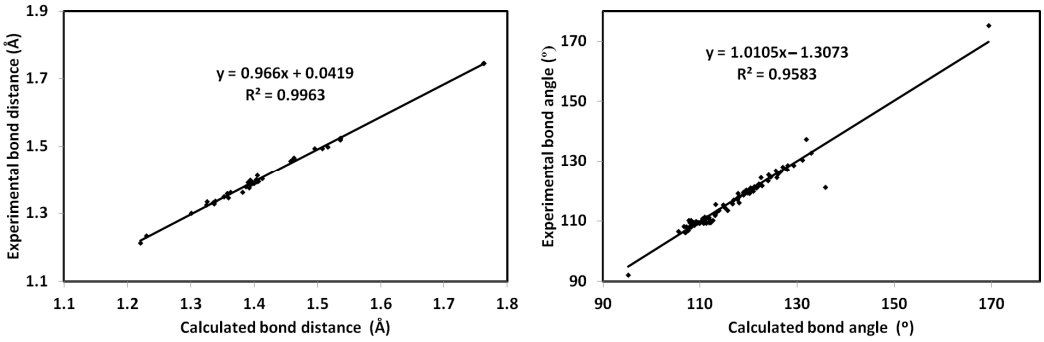

Figure 9. Correlations of the calculated and experimental geometric parameters.

The natural atomic charges are presented in Figure 10. Detailed natural charges are shown in Table S3. In general, the O, N, Cl and most of C-atoms have negative charge while the opposite is true for the hydrogen atoms and other carbon atoms bonded to oxygen and nitrogen. The compound has a net dipole moment of 5.6072 Debye indicating a highly polar system. In addition, the electron density mapped over electrostatic potential showing the negatively charged regions colored by red and the positively charged regions colored by blue is shown in Figure 8C.

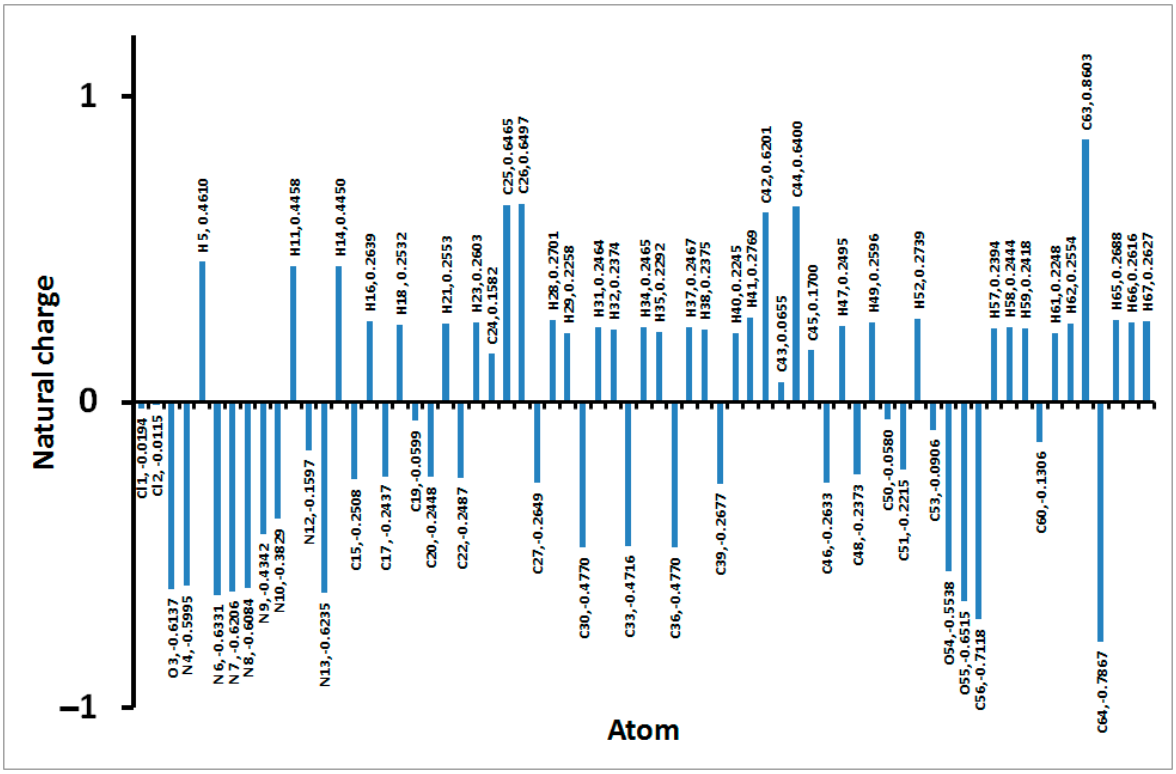

Figure 10. Charges at the different atoms based on natural population analysis.

In the same figure, the HOMO and LUMO levels are presented (Figure 8D,E). These orbitals are mainly distributed over the π-systems of the indolone and *s*-triazine moieties. The energies of these molecular orbitals are calculated to be −5.5378 and −2.3097 eV, respectively. Hence, the HOMO-LUMO energy gap is 3.2281 eV. Based on the energies of the HOMO and LUMO levels, the ionization potential (I), electron affinity (A), hardness (η), electrophilicity index (ω) and chemical potential (μ) are calculated to be 5.5378, 2.3097, 3.2281, 2.3847 and −3.9238 eV, respectively [31–37].

4. Conclusions

The present work represents the synthesis of some *s*-triazine hydrazone derivatives incorporating isatin moiety. The structure of **6c** was confirmed using X-ray diffraction of single crystal. The crystal comprised one of the organic target molecule in addition to a co-crystallized ethyl acetate as a crystal solvent. The supramolecular structure of the organic system and the crystal solvent is analyzed using Hirshfeld analysis. In the former, the molecular packing is controlled by the O . . . H (7.1%), C . . . H (16.4%), C . . . C (1.6%), H . . . H (34.8%), N . . . H (8.0%) and C . . . N (4.0%) interactions. On the other hand, the packing of the latter is dominated by O . . . H (21.3%), H . . . H (61.2%) and N . . . H (8.1%) contacts. DFT optimized geometry agreed very well with the reported X-ray structure. Different electronic and spectroscopic parameters for the studied system were predicted.

Supplementary Materials: The following supporting information can be downloaded at: https://www.mdpi.com/article/10.3390/cryst13020305/s1, Figures S1–S7: ^{1}H and ^{13}C NMR spectral data for compounds 2,3 and 6a–e: title; Table S1: Selected bond angles [°] for 6c; Table S2: The calculated geometric parameters of 6c [a] and Table S3: The calculated natural charges of 6c [a].

Author Contributions: Conceptualization, H.H.A.-R. and S.A.A.-k.; methodology, H.H.A.-R., S.M.S., M.H., A.E.-F. and A.B. software, S.M.S. and M.H.; formal analysis, H.H.A.-R., S.M.S. and M.H.; X-ray crystal structure: S.M.S. and M.H.; investigation, H.H.A.-R., S.M.S., M.H., A.E.-F. and A.B.; resources, H.H.A.-R.; writing—original draft preparation, H.H.A.-R., S.M.S., M.H., A.E.-F. and A.B.; writing—review and editing, A.E.-F., S.M.S. and A.B.; supervision, H.H.A.-R. and A.E.-F. All authors have read and agreed to the published version of the manuscript.

Funding: This research received no external funding.

Data Availability Statement: Not applicable.

Acknowledgments: All thanks and respect to Research Center of the Female Scientific and Medical Colleges, Deanship of Scientific Research, King Saud University, Saudi Arabia.

Conflicts of Interest: The authors declare no conflict of interest.

References

1. Maliszewski, D.; Drozdowska, D. Recent Advances in the Biological Activity of s-Triazine Core Compounds. *Pharmaceuticals* **2022**, *15*, 221. [CrossRef] [PubMed]
2. Aldalbahi, A.; AlOtaibi, B.S.; Thamer, B.M.; El-Faham, A. Synthesis of New S-Triazine Bishydrazino and Bishydrazido-Based Polymers and Their Application in Flame-Retardant Polypropylene Composites. *Polymers* **2022**, *14*, 784. [CrossRef] [PubMed]
3. Atta, A.M.; Ahmed, M.A.; Al-Lohedan, H.A.; El-Faham, A. Multi-Functional Cardanol Triazine Schiff Base Polyimine Additives for Self-Healing and Super-Hydrophobic Epoxy of Steel Coating. *Coatings* **2020**, *10*, 327. [CrossRef]
4. Blotny, G. Recent Applications of 2,4,6-Trichloro-1,3,5-Triazine and Its Derivatives in Organic Synthesis. *Tetrahedron* **2006**, *62*, 9507–9522. [CrossRef]
5. Gunasekaran, P.; Fan, M.; Kim, E.Y.; Shin, J.H.; Lee, J.E.; Son, E.J.; Kim, J.; Hwang, E.; Yim, M.S.; Kim, E.-H.; et al. Amphiphilic Triazine Polymer Derivatives as Antibacterial and Anti-atopic Agents in Mice Model. *Sci. Rep.* **2019**, *9*, 15161. [CrossRef]
6. Sharma, A.; Singh, S.; Utreja, D. Recent Advances in Synthesis and Antifungal Activity of 1,3,5-triazines. *Curr. Org. Synth.* **2016**, *13*, 484–503. [CrossRef]
7. Adhikari, N.; Kashyap, A.; Shakya, A.; Ghosh, S.K.; Bhattacharyya, D.R.; Bhat, H.R.; Singh, U.P. Microwave Assisted Synthesis, Docking and Antimalarial Evaluation of Hybrid PABA-Substituted 1,3,5-Triazine Derivatives. *J. Heterocyc. Chem.* **2020**, *57*, 2389–2399. [CrossRef]
8. Zacharie, B.; Abbott, S.D.; Duceppe, J.S.; Gagnon, L.; Grouix, B.; Geerts, L.; Laurin, P. Design and Synthesis of New 1,3,5-Trisubstituted Triazines for the Treatment of Cancer and Inflammation. *ChemistryOpen* **2018**, *7*, 737–749. [CrossRef]
9. Baréa, P.; Barbosa, V.A.; Bidóia, D.L.; de Paula, J.C.; Stefanello, T.F.; da Costa, W.F.; Sarragiotto, M.H. Synthesis, Antileishmanial Activity and Mechanism of Action Studies of Novel B-Carboline-1,3,5-Triazine Hybrids. *Eur. J. Med. Chem.* **2018**, *150*, 579–590. [CrossRef]
10. Barakat, A.; El-Senduny, F.F.; Almarhoon, Z.; Al-Rasheed, H.H.; Badria, F.A.; Al-Majid, A.M.; El-Faham, A. Synthesis, X-ray Crystal Structures, and Preliminary Antiproliferative Activities of New s-Triazine-hydroxybenzylidene Hydrazone Derivatives. *J. Chem.* **2019**, *2019*, 9403908. [CrossRef]
11. Shvekhgeimer, M.-G.A. Synthesis of Heterocyclic Compounds by the Cyclization of Isatin and Its Derivatives (Review). *Chem. Heterocycl. Compd.* **1996**, *32*, 249–276. [CrossRef]
12. Da Silva, J.F.M.; Garden, S.J.; Pinto, A.C. The Chemistry of Isatins: A Review from 1975 to 1999. *J. Braz. Chem. Soc.* **2001**, *12*, 273–324. [CrossRef]
13. Basedia, D.K.; Dubey, B.K.; Shrivastava, B. A Review on Synthesis and Biological Activity of Heterocyclic Compounds Bearing 1,3,5-Triazine Lead Moiety. *Am. J. Pharm. Res.* **2011**, *1*, 174–193.
14. Shen, J.; Zhang, L.; Meng, X. Recent Advances in Cyclization Reactions of Isatins or Thioisatins via C–N Or C–S Bond Cleavage. *Org. Chem. Front.* **2021**, *8*, 6433. [CrossRef]
15. Khan, F.A.; Maalik, A. Advances in Pharmacology of Isatin and its Derivatives: A Review. *Trop. J. Pharm. Res.* **2015**, *14*, 1937–1942. [CrossRef]
16. Bhrigu, B.; Pathak, D.; Siddiqui, N.; Alam, M.S.; Ahsan, W. Search for Biological Active Isatins: A Short Review. *Int. J. Pharm. Sci. Drug Res.* **2010**, *2*, 229–235.
17. Smitha, S.; Pandeya, S.N.; Stables, J.P.; Ganapathy, S. Anticonvulsant and Sedative-Hypnotic Activities of N-Acetyl/Methyl Isatin Derivatives. *Sci. Pharm.* **2008**, *76*, 621–636. [CrossRef]

18. Srivastava, G.K.; Alonso-Alonso, M.L.; Fernandez-Bueno, I.; Garcia-Gutierrez, M.T.; Rull, F.; Medina, J.; Coco, R.M.; Pastor, J.C. Comparison between Direct Contact and Extract Exposure Methods for PFO Cytotoxicity Evaluation. *Sci. Rep.* **2018**, *8*, 1425. [CrossRef]
19. Ghodsi, M.Z.; Zahra, P.; Fatemeh, M.; Mohammad, G.; Rajender, S.V. An Overview of Recent Advances in Isatin-Based Multicomponent Reactions. *Curr. Org. Chem.* **2022**, *26*, 1485–1502.
20. Yan, L.J.; Wang, Y.C. Recent Advances in Green Synthesis of 3,3′-Spirooxindoles via Isatin–based One–pot Multicomponent Cascade Reactions in Aqueous Medium. *ChemistrySelect* **2016**, *1*, 6948–6960. [CrossRef]
21. Shanmugakala, R.; Tharmaraj, P.; Sheela, C.D.; Chidambaranathan, N. Transition Metal Complexes of *S*-Triazine Derivative: New Class of Anticonvulsant, Anti-Inflammatory, and Neuroprotective Agents. *Med. Chem. Res.* **2014**, *23*, 329–342. [CrossRef]
22. Shawish, I.; Barakat, A.; Aldalbahi, A.; Malebari, A.M.; Nafie, M.S.; Bekhit, A.A.; Albohy, A.; Khan, A.; Ul-Haq, Z.; Haukka, M.; et al. Synthesis and Antiproliferative Activity of a New Series of Monoand Bis(dimethylpyrazolyl)-s-triazine Derivatives Targeting EGFR/PI3K/AKT/mTOR Signaling Cascades. *ACS Omega* **2022**, *7*, 24858–24870. [CrossRef] [PubMed]
23. Rikagu Oxford Diffraction. *CrysAlisPro*; Agilent Technologies Inc.: Oxfordshire, UK, 2018.
24. Sheldrick, G.M. *SADABS—Bruker Nonius Scaling and Absorption Correction*; Bruker AXS, Inc.: Madison, WI, USA, 2012.
25. Sheldrick, G.M. SHELXT-Integrated Space-Group and Crystal-Structure Determination. *Acta Crystallogr. Sect. A Found. Adv.* **2015**, *71*, 3–8. [CrossRef] [PubMed]
26. Hübschle, C.B.; Sheldrick, G.M.; Dittrich, B. *ShelXle*: A Qt Graphical User Interface for *SHELXL*. *J. Appl. Crystallogr.* **2011**, *44*, 1281–1284. [CrossRef] [PubMed]
27. Turner, M.J.; McKinnon, J.J.; Wolff, S.K.; Grimwood, D.J.; Spackman, P.R.; Jayatilaka, D.; Spackman, M.A. Crystal Explorer17 (2017) University of Western Australia. Available online: https://crystalexplorer.net/download/ (accessed on 1 July 2017).
28. Frisch, M.J.; Trucks, G.W.; Schlegel, H.B.; Scuseria, G.E.; Robb, M.A.; Cheeseman, J.R.; Scalmani, G.; Barone, V.; Mennucci, B.; Petersson, G.A. *GAUSSIAN 09, Revision A.02*; Gaussian Inc.: Wallingford, CT, USA, 2009.
29. Dennington, R.D., II; Keith, T.A.; Millam, J.M. *GaussView, Version 4.1*; Semichem Inc.: Shawnee Mission, KS, USA, 2007.
30. Reed, A.E.; Curtiss, L.A.; Weinhold, F. Intermolecular Interactions from A Natural Bond Orbital, Donor-Acceptor Viewpoint. *Chem. Rev.* **1988**, *88*, 899–926. [CrossRef]
31. Foresman, J.B.; Frisch, A. *Exploring Chemistry with Electronic Structure Methods*, 2nd ed.; Gaussian: Pittsburgh, PA, USA, 1996.
32. Koopmans, T.A. Ordering of WaveFunctions and Eigenenergies to the Individual Electrons of an Atom. *Physica* **1933**, *1*, 104–113. [CrossRef]
33. Parr, R.G.; Yang, W. *Density-Functional Theory of Atoms and Molecules*; Oxford University Press: New York, NY, USA, 1989.
34. Parr, R.G.; Szentpály, L.V.; Liu, S. Electrophilicity Index. *J. Am. Chem. Soc.* **1999**, *121*, 1922–1924. [CrossRef]
35. Singh, R.N.; Kumar, A.; Tiwari, R.K.; Rawat, P.; Gupta, V.P. A Combined Experimental and Quantum Chemical (DFT And AIM) Study on Molecular Structure, Spectroscopic Properties, NBO and Multiple Interaction Analysis in A Novel Ethyl 4-[2-(Carbamoyl) Hydrazinylidene]-3,5-Dimethyl-1H-Pyrrole-2-Carboxylate and Its Dimer. *J. Mol. Strut.* **2013**, *1035*, 427–440. [CrossRef]
36. Hubert Joe, I.; Kostova, I.; Ravikumar, C.; Amalanathan, M.; Pinzaru, S.C. Theoretical and Vibrational Spectral Investigation of Sodium Salt of Acenocoumarol. *J. Raman Spectrosc.* **2009**, *40*, 1033–1038.
37. Sebastian, S.; Sundaraganesan, N. The Spectroscopic (FT-IR, FT-IR Gas Phase, FT-Raman and UV) and NBO Analysis of 4-Hydroxypiperidine by Density Functional Method. *Spectrochim. Acta Part A Mol. Biomol. Spectrosc.* **2010**, *75*, 941–952. [CrossRef]